process can be described by

$$|M^{\mathbf{k}}_{f,i}| \propto |\langle \phi^{\mathbf{k}}_f | \hat{\varepsilon} \cdot \mathbf{r} | \phi^{\mathbf{k}}_{\mathbf{i}} \rangle|^{\mathbf{2}}$$

, where $\phi^{\mathbf{k}}_i$ and $\phi^{\mathbf{k}}_f$ are the initial and final state wavefunctions respectively [29]. In our experimental setup, the momentum of the final-state photoelectron is in the mirror plane, and $\phi^{\mathbf{k}}_f$ can be approximated by a plane wave. Therefore, $\phi^{\mathbf{k}}_f$ is always even with respect to the mirror plane. In the π geometry, $(\hat{\varepsilon} \cdot \mathbf{r})$ is even, to give a finite photoemission matrix element, $|\phi^{\mathbf{k}}_i\rangle$ must be even with respect to the mirror plane. Thus only even state is probed in the π experimental geometry. On the other hand, one could similarly deduce that only odd state is observed in the σ geometry.

In contrast to the data measured with circularly polarized light in Figs. 2(i) and (j), only the β band is observed in the σ geometry [Figs. 8(b) and (d)], while just the α and γ bands are observed in the π geometry [Figs. 8(c) and (e)]. Based on the symmetry of different orbitals illustrated in Fig. 8(a), the β band is odd with respect to the mirror plane, while the α and γ bands are even along the Γ-X direction. Therefore, the β band has to be made of d_{xy} and/or d_{yz} orbitals, while the α and γ bands may be consisted of $d_{x^2-y^2}$, d_{z^2}, and/or d_{xz}.

These experimental findings of the symmetry properties of the band structure are well captured by the band structure calculation. In Fig. 9, the orbital characters of the bands are shown by the false color plot. Near the Fermi energy, the α band is mainly consisted of d_{xz}/d_{yz} orbitals, which should be purely d_{xz} along the $\Gamma - X$ direction. The β band is consisted of mainly d_{xz} and d_{yz} orbitals, and some d_{xy} orbitals; while the γ band is consisted of $d_{x^2-y^2}$ orbital. Along the $\Gamma - Z$ direction, the band structure near E_F has some contributions from the p_z orbital and small contributions from the d_{z^2} orbital. They all have even symmetry and thus can be observed in the π experimental geometry. The small ellipsoidal Fermi surface near zone center is mainly contributed by the d_{z^2} orbital for FeAs-based compounds, while for $Fe(Te_{0.66}Se_{0.34})$, Te/Se p_z orbital plays an important role. To have a more quantitative picture, we have listed the contributions of various orbitals to the states at E_F in Table. I, which are the coefficients of the calculated corresponding Bloch wavefunctions projected into the orbitals.

VI. DISCUSSION

Although the chalcogen ions contribute little spectral to the density-of-states (DOS) near the Fermi energy, the Fe 3d related band structure in iron-chalcogenides does show significant difference compared with that of iron-pnictides. Recently, it is even proposed that the polarization of the As p orbitals might be the cause of the unconventional superconductivity in FeAs-based superconductors [11]. Therefore in this regard, the electronic

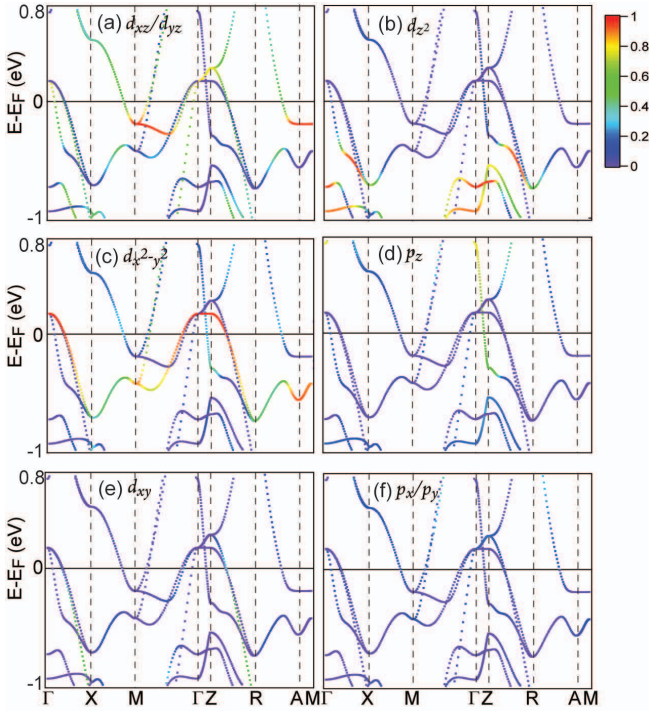

Figure 9: (color online) Contributions of various Fe 3d and Te/Se p orbitals to the calculated band structure of $Fe(Te_{0.66}Se_{0.34})$.

consequences related to the chalcogen or pnicogen anions in the iron-based superconductors are particularly interesting to explore.

In general, $Fe_{1.04}(Te_{0.66}Se_{0.34})$ has similar Fermi surface and band structure as the iron-pnictides [22, 30]. However, there are some important differences. For example, the three bands near Γ are well separated in this iron-chalcogenides, each with distinct symmetry. On the other hand in recent polarization dependence studies of the $BaFe_{1.82}Co_{0.18}As_2$, only two features around Γ were observed [22]. Moreover, the inner feature is a mixture of orbitals of both even and odd symmetries, while the outer feature is even in symmetry. Moreover, our calculations show that the Te 5p orbitals contribute to the density of states near the Fermi energy, while Fe $3d_{z^2}$ orbital contributes very little in this iron-chalcogenide. Furthermore, there is a small ellipsoidal Fermi surface near the zone center of $Fe_{1.04}(Te_{0.66}Se_{0.34})$, while for iron-pnictides, such a small Fermi pocket has not been unambiguously observed in the paramagnetic normal state.

Compared with the electronic structure of $Fe_{1+y}Te$ obtained earlier [31], the $Fe_{1.04}(Te_{0.66}Se_{0.34})$ electronic structure behaves differently in the following two aspects. First, three bands α, β, and γ, are clearly observed around Γ for $Fe_{1.04}(Te_{0.66}Se_{0.34})$, whereas only two bands were distinguished in $Fe_{1+y}Te$. Secondly, a weak Fermi surface was observed around X-point in $Fe_{1+y}Te$, which was argued to be a folded Fermi surface by the spin density wave. For $Fe_{1.04}(Te_{0.66}Se_{0.34})$, neutron scattering ex-